

Lanthanum-Neodymium-Co-Substituted Calcium Fluorobriholites

Mustapha Hidouri^{1,2}, Nawaf Albeladi³

¹Higher Institute of Applied Sciences and Technology of Gabes, Gabes University, Gabes, Tunisia

²RU Catalysis and Materials for Environment and Process, Engineering School, Gabes University, Gabes, Tunisia

³Chemistry Department, Faculty of Sciences Yanbu, Taibah University, Yanbu Al Bahr, KSA

Email: mustapha.hidouri@issatgb.rnu.tn, nawaf328@hotmail.com

How to cite this paper: Hidouri, M. and Albeladi, N. (2018) Lanthanum-Neodymium-Co-Substituted Calcium Fluorobriholites. *Journal of Materials Science and Chemical Engineering*, 6, 151-162.
<https://doi.org/10.4236/msce.2018.67016>

Received: February 16, 2018

Accepted: June 10, 2018

Published: July 31, 2018

Copyright © 2018 by authors and Scientific Research Publishing Inc.

This work is licensed under the Creative Commons Attribution International License (CC BY 4.0).

<http://creativecommons.org/licenses/by/4.0/>



Open Access

Abstract

Britholites are considered as potential matrices for storage of nuclear wastes such as minor actinides and long-lived fission byproducts. This investigation is concerned with the study of simultaneous substitution in calcium fluor-britholite framework of two lanthanide ions assimilated to radionuclides. A series of calcium fluorbritholites doped with lanthanum and neodymium $\text{Ca}_8\text{La}_{2-x}\text{Nd}_x(\text{PO}_4)_4(\text{SiO}_4)_2\text{F}_2$ with $0 \leq x \leq 2$ were prepared via a solid state reaction in the temperature range $1450^\circ\text{C} - 1250^\circ\text{C}$. The obtained products were characterized by several techniques such as Chemical analysis via Inductively coupled plasma Atomic emission spectrometry ICP-AES, X-ray diffraction (XRD), Fourier transformed infra-red spectroscopy FTIR and Nuclear magnetic resonance ^{31}P NMR (MAS). Obtained solid solutions containing lanthanum and neodymium in variable proportions were typically apatite of hexagonal structure P63/m spatial group. The stoichiometry of the powders was verified via the metal/(phosphate + silicate) molar ratios found at about 1.67. The lattice parameters a and c calculated by the Rietveld method decreased as neodymium level increased. Despite, the close respective sizes of lanthanum and neodymium ions ($^{VI}\text{r}_{\text{La}^{3+}} = 1.032\text{\AA}$, $^{VI}\text{r}_{\text{Nd}^{3+}} = 0.983\text{\AA}$), their mutual substitutions led to solid solutions in whole range of composition with preferential occupation of Me (2) sites.

Keywords

Calcium Fluorobriholites, Lanthanum-Neodymium, Ionic Substitutions

1. Introduction

Over the last decades, apatites of general formula $\text{Me}_{10}(\text{XO}_4)_6\text{Y}_2$ with Me a divalent cation, XO_4 a trivalent anion and Y a monovalent anion have acquired an

exhaustive importance because of their distinctive characteristics. Indeed, these materials have a flexible and rigid structure able to admit a large number of substitutions both cationic and anionic total or limited with unchanged crystallographic structure [1] [2] [3]. In addition, these materials are endowed with chemical and thermal stability and low solubility, they also have interesting mechanical properties [4] [5] [6] [7] [8]. All of these specifications allow these materials to be used in various fields such as chemical industry where the apatite ores are the main source of phosphate fertilizers and they are also used in phosphoric acid and various phosphate derivatives industry [9]. A further use of apatites is in optics [10] [11], in pharmaceuticals (excipient) and in chromatography (column) [12] [13] or as materials for laser [14].

Currently, calcium phosphate apatites are frequently used in orthopedic and dentistry surgery as a substitute for failing bones and teeth [15] [16] [17] [18]. These compounds have shown interesting properties of bioactivity and osteoconduction as well as a chemical composition and a crystal structure similar to that of the mineral part of calcified tissue [19] [20] [21]. Apatites are particularly studied as electrolyte for solid oxide fuel cells (SOFC) [22]. Recently, new applications in the field of the environment have appeared; apatitic derivatives with coupled substitutions of divalent cations by rare earth elements (lanthanides: Ln^{3+} or actinides: Ac^{3+}) and the silicates SiO_4^{4-} partially substitute XO_4 groups. Such a family, called britholites, acted as a matrix for conditioning certain radionuclides and heavy metals [23] [24] [25]. However, it has been shown that the natural nuclear reactors Alko of Gabon contain britholites which immobilize radionuclide like cesium as well as minor actinides [26] [27]. Consequently, several studies have been conducted in order to better valorize the retention capacity of these elements by this family of apatites.

The apatitic structure crystallizing in the hexagonal system, space group P63/m [28] [29], is built on a skeleton formed of parallel layers of XO_4 ions arranged in a hexagonal way and giving rise to two types of tunnels where the metal ions Me are localized. As shown in **Figure 1**, these ions are distributed between two non-equivalent crystallographic sites. The Me (1) sites, also called 4f, four in number, are aligned in columns along the ternary axis c and surrounded by nine oxygen atoms. The six other Me (2) sites, called 6 h, six in number, were organized at the top of two equilateral triangles centered on the helicoidally axis (**Figure 1**). Me (2) sites are coordinated with six oxygen atoms

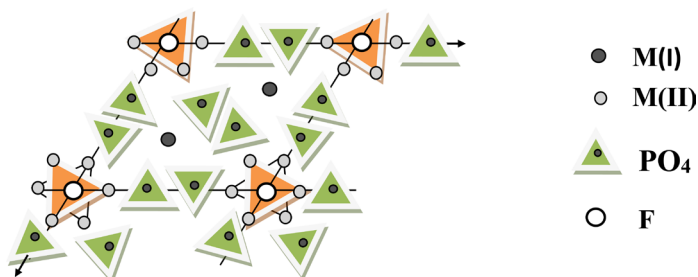


Figure 1. Perspective view of the fluorapatite structure [30].

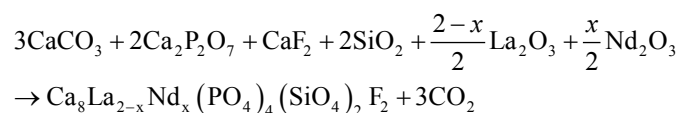
and one Y ion. Thus, calcium can be substituted by many mono, di or trivalent ions. Thereby, these cationic substitutions strongly depend on the difference in ionic radii, the valence, the electronegativity as well as the polarizability of the ions [31].

An earlier spectroscopic and structural study of $\text{Ca}_{10-x}\text{La}_x(\text{PO}_4)_{6-x}(\text{SiO}_4)_x\text{F}_2$ showed that the composition $x = 2$ is stable and the coupled substitutions of lanthanum by calcium and silicates by phosphates have occurred without structural modification [32]. The present work consists in studying the simultaneous substitution of lanthanum by neodymium in the designated composition $x = 2$. A series of compounds $\text{Ca}_8\text{La}_{2-x}\text{Nd}_x(\text{PO}_4)_4(\text{SiO}_4)_2\text{F}_2$ with $0 \leq x \leq 2$ should be investigated.

2. Experimental Process

2.1. Preparation and Synthesis of Powders

Britholitic powders $\text{Ca}_8\text{La}_{2-x}\text{Nd}_x(\text{PO}_4)_4(\text{SiO}_4)_2\text{F}_2$ with $0 \leq x \leq 2$ were prepared by solid state reaction using 1.8×10^{-3} moles of calcium fluoride CaF_2 (99.99% Merck), 4.54×10^{-3} moles of calcium carbonate CaCO_3 ($\geq 99.0\%$ Fluka), 3×10^{-3} moles of silica SiO_2 (Prolabo) and Calcium diphosphate $\text{Ca}_2\text{P}_2\text{O}_7$, lanthanum oxides La_2O_3 (99.999% Merck) and neodymium oxide Nd_2O_3 (99.99% Merck) whose molar quantities are given in **Table 1**. The formation reaction is as follow:



The preparation of $\text{Ca}_2\text{P}_2\text{O}_7$ is similar to that of $\text{Sr}_2\text{P}_2\text{O}_7$ strontium diphosphate previously described [29]. All the reagents were mixed in stoichiometric amounts to obtain 1.5×10^{-3} moles of each final product. The solid mixture of reagents was homogenized by prolonged grinding in an agate mortar and then cold pelletized at 100 MPa. The pellets were firstly treated at 900°C for 12 hours then thrice milled, homogenized and repelletized for heat treatments during 12hours in the range $1450^\circ\text{C} - 1250^\circ\text{C}$ with a decreased temperature of 50°C for each x value. All specimens will be afterwards abbreviated according to the index that bears the La^{3+} and Nd^{3+} ions as CaLa_2F , $\text{CaLa}_{1.5}\text{Nd}_{0.5}\text{F}$, $\text{CaLa}_1\text{Nd}_1\text{F}$, $\text{CaLa}_{0.5}\text{Nd}_{1.5}\text{F}$ and CaNd_2F .

2.2. Characterization of Powders

Several techniques were employed for the characterization of synthesized powders; X-ray diffraction were performed using a PRO PANALYTICAL X'pert PRO

Table 1. Number of moles of lanthanum and neodymium oxides used in the synthesis of fluorbritholites $\text{Ca}_8\text{La}_{2-x}\text{Nd}_x(\text{PO}_4)_4(\text{SiO}_4)_2\text{F}_2$ with $0 \leq x \leq 2$.

Reagents	SrLa_2F	$\text{SrLa}_{1.5}\text{Nd}_{0.5}\text{F}$	$\text{SrLa}_1\text{Nd}_1\text{F}$	$\text{SrLa}_{0.5}\text{Nd}_{1.5}\text{F}$	SrNd_2F
La_2O_3	1.5×10^{-3}	1.12×10^{-3}	0.75×10^{-3}	0.37×10^{-3}	-
Nd_2O_3	-	0.37×10^{-3}	0.75×10^{-3}	1.12×10^{-3}	1.5×10^{-3}

apparatus using K α copper Cu radiation ($\lambda = 1.5406 \text{ \AA}$). The collections are recorded in 2θ mode in the angular range $20^\circ - 80^\circ$ with a counting speed of $0.02^\circ \text{ s}^{-1}$. The crystalline phases have been identified by comparison with JCPDS files (Joint Committed Powder Diffraction Standard). The lattices parameters a and c of each sample were calculated by the Rietveld method using the Fullprof program. The FTIR spectra were recorded from 400 to 4000 cm^{-1} on a Perkin Elmer spectrometer and recorded data were in ATR (Attenuated Total Reflectance) mode based on material reflectance. ^{31}P NMR-MAS spectra were recorded on a BRUKER MSL 300 spectrometer operating at Larmor frequency of 121.44 MHz for phosphorus. Spinning rate of the sample at the magic angle was 8 KHz . Chemical shifts were measured against tetramethylsilane (TMS) as a reference material. The amounts of chemical elements present in each synthesized sample were determined by inductively coupled plasma atomic emission spectrometry (ICP-AES) using a Shimadzu 9800 series apparatus while that of fluoride was measured potentiometrically by a specific ion-selective electrode.

3. Results and Discussion

The identification of crystalline phases was determined by examination of obtained diffractograms of synthesized powders given in **Figure 2**. Hence, their indexation was made with reference to the $\text{Ca}_{10}(\text{PO}_4)_6\text{F}_2$ phase (JCPDS card 01-076-0558), shows that the different synthesized samples are characteristic of a single-phase apatite with hexagonal symmetry spatial group P63/m. Therefore, due to the limited sensitivity of the DRX technique, no secondary phase has been detected. However, small amounts (less than 2%) of impurities may be present.

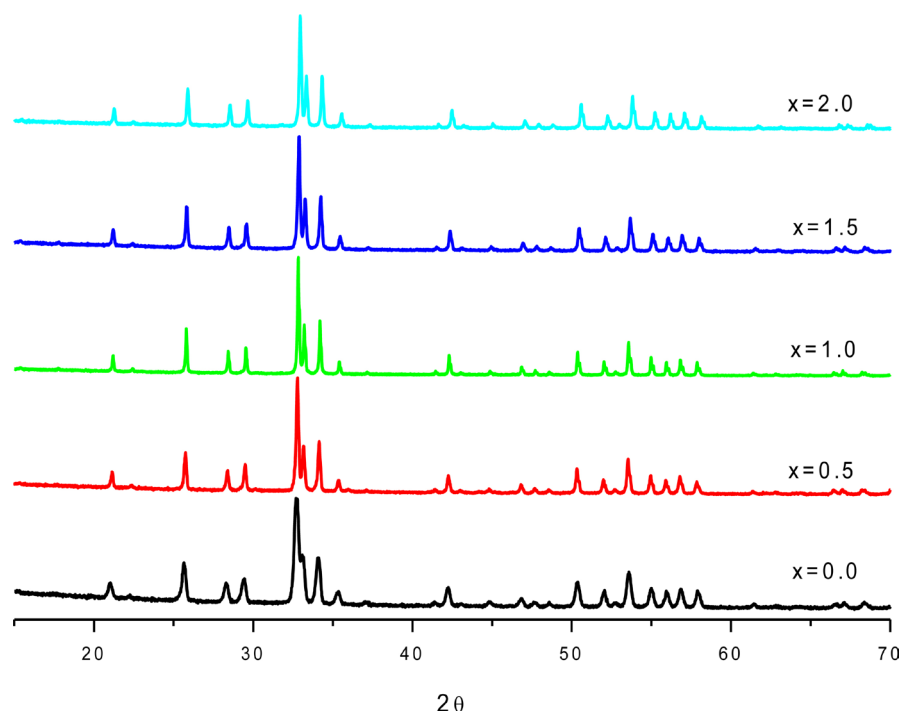


Figure 2. DRX diffractograms of fluorbritholites $\text{Ca}_8\text{La}_{2-x}\text{Nd}_x(\text{PO}_4)_4(\text{SiO}_4)_2\text{F}_2$ ($0 \leq x \leq 2$).

Despite the size of lanthanum (${}^{\text{VI}}r_{\text{La}^{3+}} = 1.032 \text{ \AA}$) slightly higher than that of neodymium (${}^{\text{VI}}r_{\text{Nd}^{3+}} = 0.983 \text{ \AA}$) [33], the solid solution doped with lanthanum and neodymium was formed and the substitution was in whole range. The slight displacement of the radiations (300) towards the higher diffraction angles confirm that the substitution of lanthanum by neodymium occurred (Figure 3) and that all the neodymium introduced at the starting solutions substituted lanthanum. The lines of the composition $x = 1$ showed a diffraction lines doubling which is probably related to the slight phase transition and slightly affected the symmetry of the crystalline structure. It may be caused either by the cationic substitution or by the thermal treatments during synthesis.

The calculated lattice parameters a and c presented in Figure 4 showed particularly a significant decrease of these parameters as the level of substituted Nd^{3+} increased. All obtained values given in Table 2 are similar to that of calcium britholites [34]. These parameters as well as the volume of the lattice decreased when the level of introduced neodymium increased in agreement with its small size compared to that of lanthanum. As shown in Figure 4, the lattice parameters a and c vary linearly with the substitution level x according to Végard's law and satisfy the following equations:

$$a = -0.0122x + 9.5006 \text{ \AA}; \sigma(x) = 2.5 \times 10^{-3} \text{ \AA} \quad (\sigma: \text{standard deviation})$$

$$c = -0.0156x + 7.2888 \text{ \AA}; \sigma(x) = 2 \times 10^{-3}$$

Consequently, the volume presented a linear decrease (Figure 4) according to the following equation:

$$v = -2.176x + 569.22 \text{ \AA}^3; \sigma(x) = 10^{-3} \text{ \AA}^3$$

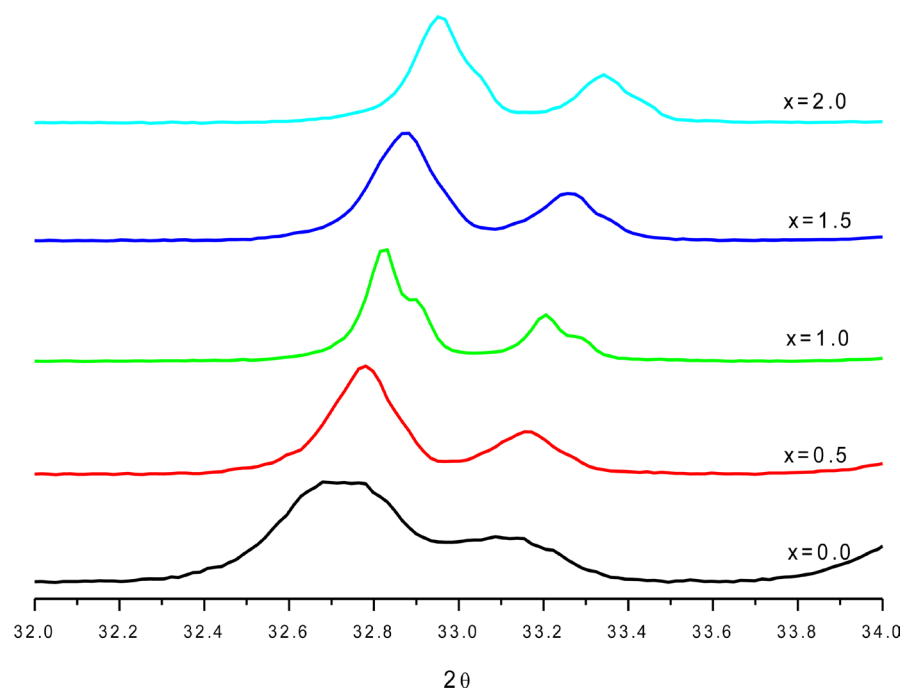


Figure 3. Radiation (300) of fluorbritholites $\text{Ca}_8\text{La}_{2-x}\text{Nd}_x(\text{PO}_4)_4(\text{SiO}_4)_2\text{F}_2$ ($0 \leq x \leq 2$).

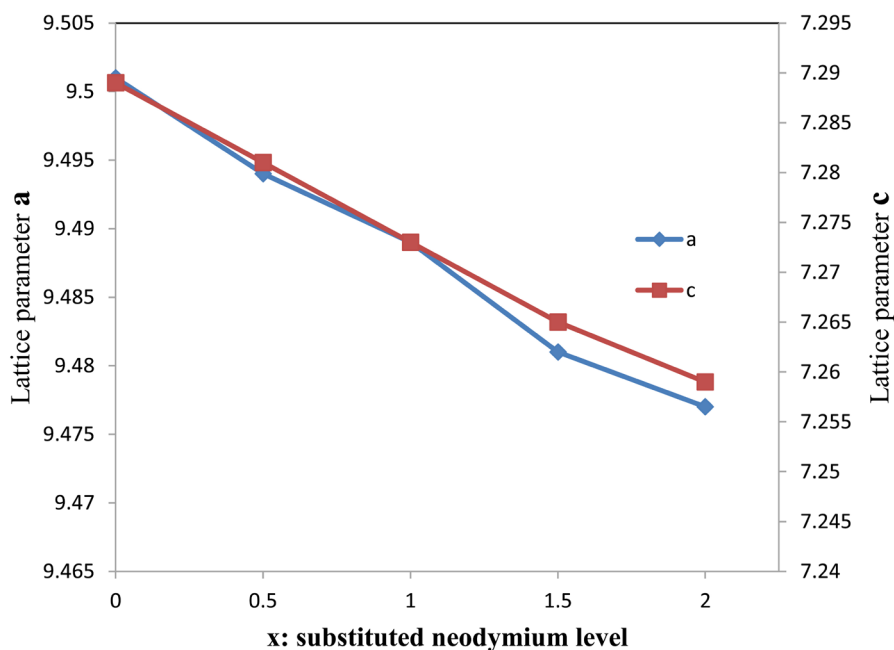


Figure 4. Variation of lattices parameters as a function neodymium level in the $\text{Ca}_8\text{La}_{2-x}\text{Nd}_x(\text{PO}_4)_4(\text{SiO}_4)_2\text{F}_2$ ($0 \leq x \leq 2$).

Table 2. Lattices parameters (Å) and volume of fluorbritholites $\text{Ca}_8\text{La}_{2-x}\text{Nd}_x(\text{PO}_4)_4(\text{SiO}_4)_2\text{F}_2$ ($0 \leq x \leq 2$).

x	a	c	V (Å ³)
0.0	9.501(2)	7.289(2)	569.11(2)
0.5	9.494(1)	7.281(2)	568.35(2)
1.0	9.489(2)	7.273(3)	567.13(3)
1.5	9.481(3)	7.265(2)	565.55(3)
2.0	9.477(2)	7.259(4)	564.61(4)

Many studies were interested to the repartition of the lanthanide ions between the two cationic sites of the calcium britholites structure. It was confirmed that the occupancy factors relative to substituted lanthanides depends on many factors particularly on the tunnel anions nature (PO_4^{3-} , SiO_4^{4-} , ...), the substitution level as well as the Y^- nature (F^- , Cl^- , Br^- , ...) [34] [35] [36] [37] [38]. Briefly, when La^{3+} substituted calcium in lower amounts (~ 2 atom/unit cell), the ions were located into the two sites with strong preference to occupy Me (2) sites. Whereas with higher substituted amounts the repartition became statistical between the two sites. In case of double substitution of calcium by lanthanum and neodymium with a rate inferior or equal to two and due to similarity of the substituting ions they should occupy the Me (2) sites. The preferential occupation of the two ions in Me (2) sites is coherent with the ionic radius of Ca^{2+} (${}^{\text{VI}}r_{\text{Ca}^{2+}} = 1.14 \text{ \AA}$) slightly superior to that of lanthanide ions meanwhile with inferior ionic radius like strontium Sr^{2+} the preference of localization in Me (2) also exist. Hence, the parameters other than the ionic sizes such as electronega-

tivity, valence and polarizability are responsible for the two sites occupations. When the electronegativities of the ions were 1.00, 1.10 and 1.14 for Ca^{2+} , La^{3+} and Nd^{3+} , respectively. These values considered once again as similar lead to think that the valence and polarizabilities were the remaining relevant parameter for the preferential occupation of Me (2) sites. This was verified with the ions polarizabilities values, expressed in \AA^3 , found significantly different (Ca^{2+} :1.91; La^{3+} :4.45; Nd^{3+} :4.20) as well as the valence difference between calcium and the lanthanides. Therefore, a non-radioactive analogues to minor actinides were conditioned in calcium-fluorbritholite matrix.

In order to determine the content of each element in the synthesized powders, to verify the stoichiometry and to establish the formulas of the prepared phases, all samples were chemically analyzed. The results summarized in **Table 3** are comparable with the expected values showing that the amounts of neodymium rise whereas those of lanthanum decrease verifying once again that all of the Nd^{3+} added to the starting solution completely reacted and substituted those of La^{3+} . The stoichiometry of the powders verified by comparison with the theoretical ratio $\frac{\text{Me}}{\text{P} + \text{Si}}$ equal to 1.67 was determined by $\frac{\text{Ca} + \text{La} + \text{Nd}}{\text{P} + \text{Si}}$ molar ratios. The values shown in **Table 3** were slightly lower than the stoichiometric value. Experimental errors may be responsible for this small difference in stoichiometry values. This should indicate eventually, that the substitution of lanthanum by neodymium in the apatite structure slightly affected the powders stoichiometry. Finally, the amount of fluoride contained in powders was very close to that of the starting solutions highlighting electroneutrality of chemical formulas.

The infrared absorption spectra of fluorbritholites $\text{Ca}_8\text{La}_{2-x}\text{Nd}_x(\text{PO}_4)_4(\text{SiO}_4)_2\text{F}_2$ with ($0 \leq x \leq 2$) are shown in **Figure 5**. Their attributions were made by comparison with the spectra of the $\text{Sr}_8\text{La}_2(\text{PO}_4)_4(\text{SiO}_4)_2\text{F}_2$ phase [30]. The spectra show that apart from the PO_4 vibrational modes, those of the SiO_4 and this was in an apatitic environment [39]. The characteristic bands associated to PO_4 as well as their vibration mode are as follows; The band range $1056 - 1028 \text{ cm}^{-1}$ corresponding to the asymmetric stretching mode (ν_3), the band at 954 cm^{-1} is relative to the symmetrical stretching mode (ν_1). Bands at $544 - 585 \text{ cm}^{-1}$ range and at 454 cm^{-1} were respectively assigned to asymmetric bending mode (ν_4)

Table 3. Chemical composition in $\text{mmol}\cdot\text{g}^{-1}$ of the as prepared powders of fluorbritholites $\text{Ca}_8\text{La}_{2-x}\text{Nd}_x(\text{PO}_4)_4(\text{SiO}_4)_2\text{F}_2$ with ($0 \leq x \leq 2$).

x	Ca	La	Nd	P	Si	F	$\frac{\text{Ca} + \text{La} + \text{Nd}}{\text{P} + \text{Si}}$ Molar ratio
0.0	7.96 (3)	1.98 (3)	-	3.98 (3)	1.99 (3)	1.99 (3)	1.664 (3)
0.5	7.98 (2)	1.47 (3)	0.46 (2)	3.99 (3)	1.98 (3)	2.01 (2)	1.659 (3)
1.0	7.97 (3)	0.98 (2)	0.99 (2)	3.98 (2)	1.98 (3)	1.96 (2)	1.667 (2)
1.5	7.99 (3)	0.47 (3)	1.46 (3)	3.99 (3)	1.99 (2)	1.97 (3)	1.658 (3)
2.0	7.98 (2)	-	1.96 (2)	3.98 (3)	1.99 (3)	1.97 (2)	1.664 (2)

and symmetric one (ν_2). The typical SiO_4 bands were observed at 926 - 960 (ν_3), 848 - 870 (ν_1), about 550 (ν_4) and 460 - 498 cm^{-1} (ν_2). However, as shown in the spectra (Figure 3), with the increased neodymium level a shifting toward lower absorption bands of both PO_4 and SiO_4 occurred. This could be related to the reduced size of the lattice inducing an increase in anion-anion repulsion (PO_4 vs SiO_4) [40]. This result is consistent with those obtained by diffraction of X-rays and confirms that the doping with neodymium reduced lattice size.

^{31}P NMR-MAS spectroscopy analysis of various samples is shown in Figure 6.

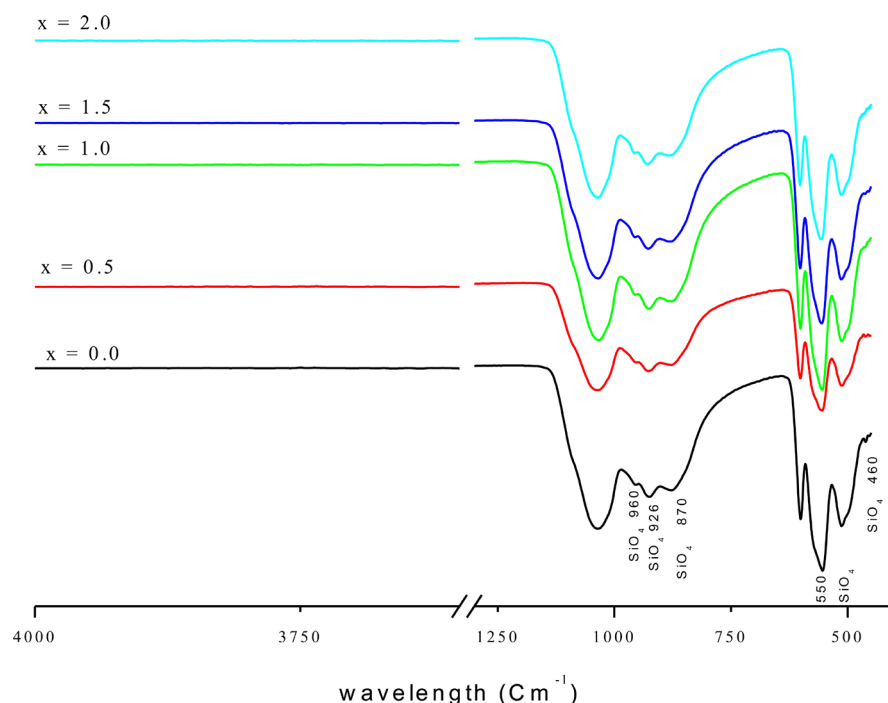


Figure 5. FTIR-ATR Spectra of fluorbritholites $\text{Ca}_8\text{La}_{2-x}\text{Nd}_x(\text{PO}_4)_4(\text{SiO}_4)_2\text{F}_2$ with ($0 \leq x \leq 2$).

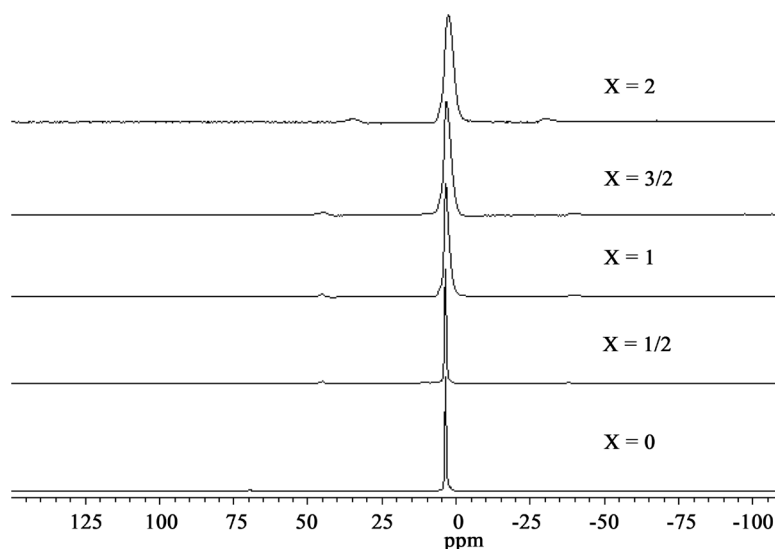


Figure 6. ^{31}P NMR-MAS spectra of fluorbritholites $\text{Ca}_8\text{La}_{2-x}\text{Nd}_x(\text{PO}_4)_4(\text{SiO}_4)_2\text{F}_2$ with ($0 \leq x \leq 2$).

Table 4. Chemical shifts δ_{iso} and FWHM (± 0.01 ppm) of PO_4 signals.

X	δ_{iso}	$\Delta\nu$ (ppm)
0.0	2.68	0.79
0.5	2.66	0.82
1.0	2.58	0.85
1.5	2.55	0.80
2.0	2.47	0.93

The spectra indicated the existence of a single isotropic peak revealing the presence of a one phosphorus type in the apatitic environment. This is coherent with the results obtained by DRX and IR showing a single apatite phase. Besides, as shown in **Table 4**, the isotropic signal was shifted and expanded with increasing neodymium content. This can be accounted for the heterogeneity of the PO_4 environment related to the incorporation of neodymium into the apatite structure. The weak enlargement of ^{31}P NMR signal is also related to neodymium substitution.

3. Conclusion

Compounds of the fluorbritholites $Ca_8La_{2-x}Nd_x(PO_4)_4(SiO_4)_2F_2$ with ($0 \leq x \leq 2$) were prepared by solid state reaction. The chemical molar ratios $\frac{Ca + La + Nd}{P + Si}$

of each composition close to the 1.67 prove that all the powders were stoichiometric. Characterization by X-ray diffraction, IR and ^{31}P NMR-MAS spectroscopy revealed that all the powders are of apatite character. The shifting in XRD radiation, in IR bands and ^{31}P NMR peaks confirmed that lanthanum-neodymium substitution occurred in whole range of composition. The lattice parameters a and c as well as the lattice of the unit cell decreased as the Nd^{3+} increased coherently to the size of the two trivalent ions. The lanthanide ions preferentially occupy Me (2) sites. Hence, the ability of these materials to confine radionuclides was evident, remains to determine precisely the rate of each element that the britholitic matrix can store. Such a study needed to be deeply investigated in coming works.

Acknowledgements

The authors gratefully acknowledge Mrs Mounira Khelifi for her help with English.

Conflicts of Interest

The authors declare no conflicts of interest regarding the publication of this paper.

References

- [1] Elliot, J.C. (1994) Structure and Chemistry of the Apatites and Other Calcium Or-

- thophosphates. *Studies in Inorganic Chemistry*, **18**, 63-94.
- [2] LeGeros, R.Z. (1994) Biological and Synthesized Apatites, In: Brown P.W., Constantz, B., Eds., *Hydroxyapatite and Related Materials*, CRC Press, Boca Raton, 3-28.
- [3] Pan, Y. and Fleet, M.E. (2002) Compositions of the Apatite-Group Minerals: Substitution Mechanisms and Controlling Factors. In: Kohn, M.J., Rakovan, J. and Hughes, J.M., Eds., *Phosphates: Geochemical, Geobiological and Material Importance, Reviews in Mineralogy and Geochemistry*, Vol. 48, Mineralogical Society of America, Washington DC, 13-50. <https://doi.org/10.2138/rmg.2002.48.2>
- [4] Ducheyne, P., Radin, S. and King, L. (1993) The Effect of Calcium Phosphate Ceramic Composition and Structure on *in Vitro* Behavior. I. Dissolution. *Journal of Biomedical Materials Research*, **27**, 25-34. <https://doi.org/10.1002/jbm.820270105>
- [5] Raynaud, S., Champion, E., Bernache-Assollant, D. and Thomas, P. (2002) Calcium Phosphate Apatites with Variable Ca/P Atomic Ratio I. Synthesis, Characterisation and Thermal Stability of Powders. *Biomaterials*, **23**, 1065-1072. [https://doi.org/10.1016/S0142-9612\(01\)00218-6](https://doi.org/10.1016/S0142-9612(01)00218-6)
- [6] Hidouri, M., Boughzala, K., Lecompte, J.P. and Bouzouita, K. (2009) Frittage et propriétés mécaniques de fluorapatites substituées au magnésium. *Comptes Rendus Physique*, **10**, 242-248. <https://doi.org/10.1016/j.crhy.2009.04.001>
- [7] Chu, T.G., Orton, D.G., Hollister, S.J., Feinberg, S.E. and Halloran, J.W. (2002) Mechanical and *in Vivo* Performance of Hydroxyapatite Implants with Controlled Architectures. *Biomaterials*, **23**, 1283-1293. [https://doi.org/10.1016/S0142-9612\(01\)00243-5](https://doi.org/10.1016/S0142-9612(01)00243-5)
- [8] Ruseska, G., Fidanceska, E. and Bossert, J. (2006) Mechanical and Thermal-Expansion Characteristics of $\text{Ca}_{10}(\text{PO}_4)_6(\text{OH})_2\text{-Ca}_3(\text{PO}_4)_2$. *Science of Sintering*, **38**, 245-254. <https://doi.org/10.2298/SOS0603245R>
- [9] Harben, P.W. and Kuzavart, M. (1996) Industrial Minerals. A Global Geology. Industrials Information Ltd. Metal Bulletin, PLC London, 409.
- [10] Becker, P., Libowitzky, E., Kleinschrodt, R. and Bohat'ý, L. (2016) Linear Optical Properties and Raman Spectroscopy of Natural Fluorapatite. *Crystal Research Technology*, **51**, 282-289. <https://doi.org/10.1002/crat.201500341>
- [11] Butler, K.H. (1980) Fluorescent Lamp Phosphors, Technology and Theory, The Pennsylvania State University Press, University Park, PA, 261.
- [12] Lin, C.-Y., Lu, Y.-T. and Liu, D.-M. (2004) Stable and Taste Masked Pharmaceutical Dosage from Using Poursous Apatite Grains. Patent Application Publication, Koslow Technologies Corporation.
- [13] Dattolo, L., Keller, E.L. and Carta, G. (2010) pH Transients in Hydroxyapatite Chromatography Columns-Effects of Operating Conditions and Media Properties. *Journal of Chromatography. A*, **1217**, 7573-7578. <https://doi.org/10.1016/j.chroma.2010.10.026>
- [14] DeLoach, L.D., Payne, S.A., Smith, L.K., Kway, W.L. and Krupke, W.F. (1994) Laser and Spectroscopic Properties of $\text{Sr}_5(\text{PO}_4)_3\text{F:Yb}$. *Journal of the Optical Society of America B*, **11**, 269-276. <https://doi.org/10.1364/JOSAB.11.000269>
- [15] Habraken, W., Habibovic, P., Epple, M. (2016) Calcium Phosphates in Biomedical Applications: Materials for the Future? *Materials Today*, **19**, 69-87. <https://doi.org/10.1016/j.mattod.2015.10.008>
- [16] Bohner, M. (2000) Calcium Orthophosphates in Medicine: From Ceramics to Calcium Phosphate Cements. *Injury*, **31**, 37-47.

- [https://doi.org/10.1016/S0020-1383\(00\)80022-4](https://doi.org/10.1016/S0020-1383(00)80022-4)
- [17] Wopenka, B. and Pasteris, J.D. (2005) A Mineralogical Perspective on the Apatite in Bone. *Materials Science and Engineering: C*, **25**, 131-143.
<https://doi.org/10.1016/j.msec.2005.01.008>
- [18] Jabr Al-Sanabani, S., Madfa, A.A. and Al-Sanabani, F.A. (2013) Application of Calcium Phosphate Materials in Dentistry. *International Journal of Biomaterials*, **2013**, Article ID: 876132.
- [19] Dorozhkin, S.V. (2016) Calcium Orthophosphate-Based Bioceramics and Biocomposites. Wiley-VCH, Weinheim, 405.
<https://doi.org/10.1002/9783527699315>
- [20] Bongio, M., Van den Beucken, J.J.J.P. and Leeuwenburgh, S.C.G. (2010) Development of Bone Substitute Materials: From "Biocompatible" to "Instructive". *Journal of Materials Chemistry*, **20**, 8747-8759. <https://doi.org/10.1039/c0jm00795a>
- [21] Landi, E., Sprio, S., Sandri, M., Celotti, G. and Tampieri, A. (2007) Development of Sr and CO₃ Co-Substituted Hydroxyapatites for Biomedical Applications. *Acta Biomaterialia*, **4**, 656-663. <https://doi.org/10.1016/j.actbio.2007.10.010>
- [22] Panteix, P.J., Julien, I., Bernache-Assollant, D. and Abélard, P. (2006) Synthesis and Characterization of Oxide Ions Conductors with the Apatite Structure for Intermediate Temperature SOFC. *Materials Chemistry and Physics*, **95**, 313-320.
<https://doi.org/10.1016/j.matchemphys.2005.06.040>
- [23] Campayo, L. (2003) Incorporation du Cesium dans des phosphates de structure apatitique et rhabdophane. Application au conditionnement des radionucléides séparés. Thèse de doctorat, Université de Limoges.
- [24] Meis, C., Gale, J.D., Boyer, L., Carpena, J. and Gosset, D. (2000) Theoretical Study of Pu and Cs Incorporation in a Mono-Silicate Neodymium Fluoroapatite Ca₉Nd(SiO₄)(PO₄)₅F₂. *The Journal of Physical Chemistry A*, **104**, 5380-5387.
<https://doi.org/10.1021/jp000096j>
- [25] Sugiyama, S. and Hayashi, H. (2003) Role of Hydroxide Groups in Hydroxyapatite Catalysts for the Oxidative Dehydrogenation of Alkanes. *International Journal of Modern Physics B*, **17**, 1476-1481. <https://doi.org/10.1142/S0217979203019186>
- [26] Carpena, J. and Sère, V. (1995) From the Natural to the Synthetic Analogue: Interest of Oklo for the Synthesis of Stable Crystalline Matrices. *Proceeding 4th Joint EC-CEA Final Meeting*, Saclay, 225.
- [27] Carpena, J., Kienast, J.R., Ouzegane, K. and Jehano, C. (1988) Evidence of the Contrasted Fission-Track Clock Behavior of the Apatites from in Ouzal Carbonatites (Northwest Hoggar): The Low-Temperature Thermal History of an Archean Basement. *Geological Society of America Bulletin*, **100**, 1237-1243.
[https://doi.org/10.1130/0016-7606\(1988\)100<1237:EOTCFT>2.3.CO;2](https://doi.org/10.1130/0016-7606(1988)100<1237:EOTCFT>2.3.CO;2)
- [28] Elliott, J.C., Wilson, R.M. and Dowker, S.E.P. (2002) Apatite Structures. Copyright (c) JCPDS-International Centre for Diffraction. *Advances in X-Ray Analysis*, Volume 45, International Centre for Diffraction Data.
- [29] Sudarsanan, K. and Young, R.A. (1969) Significant Precision in Crystal Structural Details. Holly Springs hydroxyapatite. *Acta Crystallographica Section B Structural Crystallography and Crystal Chemistry*, **25**, 1534-1543.
<https://doi.org/10.1107/S0567740869004298>
- [30] Zhua, K., Yanagisawa, K., Shimanouchi, R., Ondaa, A. and Kajiyoshi, K. (2006) Preferential Occupancy of Metal Ions in the Hydroxyapatite Solid Solutions Synthesized by Hydrothermal Method. *Journal of the American Ceramic Society*, **26**, 509-513.

- [31] Boughzala, K., Hidouri, M., Ben Salem, E., BenChrifa, A. and Bouzouita, K. (2007) Insertion du cesium dans des britholites au strontium. *Comptes Rendus Chimie*, **10**, 1137-1146. <https://doi.org/10.1016/j.jeurceramsoc.2005.07.019>
- [32] Boughzala, K., Hidouri, M., Ben Salem, E., BenChrifa, A. and Bouzouita, K. (2007) Insertion du cesium dans des britholites au strontium. *Comptes Rendus Chimie*, **10**, 1137-1146. <https://doi.org/10.1016/j.crci.2007.06.010>
- [33] Shannon, R.D. (1976) Revised Effective Ionic Radii and Systematic Studies of Interatomic Distances in Halides and Chalcogenides. *Acta Crystallographica Section A*, **32**, 751-767. <https://doi.org/10.1107/S0567739476001551>
- [34] Njema, H., Boughzala, K., Boughzala, H. and Bouzouita, K. (2013) Structural Analysis by Rietveld Refinement of Calcium and Lanthanum Phosphosilicate Apatites. *Journal of Rare Earths*, **31**, 897-904. [https://doi.org/10.1016/S1002-0721\(12\)60376-7](https://doi.org/10.1016/S1002-0721(12)60376-7)
- [35] Schroeder, L.W. and Mathew, M. (1978) Cation Ordering in $\text{Ca}_2\text{La}_8(\text{SiO}_4)_6\text{O}_2$. *Journal of Solid State Chemistry*, **26**, 383-387. [https://doi.org/10.1016/0022-4596\(78\)90173-1](https://doi.org/10.1016/0022-4596(78)90173-1)
- [36] Fleet, M.E. and Pan, Y. (1994) Site Preference of Nd in Fluorapatite $[\text{Ca}_{10}(\text{PO}_4)_6\text{F}_2]$. *European Journal of Solid State and Inorganic Chemistry*, **111**, 78. <https://doi.org/10.1006/jssc.1994.1268>
- [37] Fleet, M.E., Liu, X. and Pan, Y. (2000) Rare-Earth Elements in Chlorapatite $[\text{Ca}_{10}(\text{PO}_4)_6\text{Cl}_2]$: Uptake, Site Preference and Egradation of Monoclinic Structure. *American Mineralogist*, **85**, 1437-1446. <https://doi.org/10.2138/am-2000-1012>
- [38] Ardhaoui, K., Roger, J., Benchrifa, A., Jemal, M. and Satre, P. (2006) Standard Enthalpy of Formation of Lanthanum Oxybritholites. *Journal of Thermal Analysis and Calorimetry*, **86**, 553-559. <https://doi.org/10.1007/s10973-005-7369-1>
- [39] Boughzala, K., Ben Salem, E., Ben Chrifa, A., Gaudin, E. and Bouzouita, K. (2007) Synthesis and Characterization of Strontium-Lanthanum Apatites. *Materials Research Bulletin*, **42**, 1221-1229. <https://doi.org/10.1016/j.materresbull.2006.10.016>
- [40] Fowler, B.O. (1974) Infrared Studies of Apatites. I. Vibrational Assignments for Calcium, Strontium, and Barium Hydroxyapatites Utilizing Isotopic Substitution. *Inorganic Chemistry*, **13**, 194-207. <https://doi.org/10.1021/ic50131a039>